 DOI: 10.1002/masy.200750111

Effect of Morphology on the Relaxation Processes and Mechanical Properties in Polyimide/Silica Hybrids

Giuseppe Ragosta, Pellegrino Musto, Mario Abbate, Pietro Russo, Gennaro Scarinzi*

Summary: Polyimide/silica hybrids were produced by a sol-gel process and were examined in terms of their morphology, dynamic-mechanical properties and mechanical performances. Two types of morphology were obtained by tailoring the composition of the precursor solution mixture, i.e. phase- separated or co-continuous systems. These morphologies were found to exhibit considerably different properties. In particular, co-continuous nanocomposite systems were found much more effective in suppressing molecular relaxation processes than micron sized particulate hybrids. The latter systems, on the other hand, exhibited enhanced ductility and fracture toughness

Keywords: hybrids; mechanical properties.; morphology; relaxation processes

Introduction

Polyimides (PI) are a class of representative high-performance polymers possessing the cyclic imide and aromatic groups in the main chains. They have gained considerable importance in sectors such as microelectronics, aerospace and separation technologies owing to their outstanding properties in terms of thermal stability, mechanical properties, and solvent resistance, coupled with relatively low permittivity and dielectric losses up to very high temperatures.[1–3] In order to facilitate progress of PIs in their application fields, much effort has been spent to further improve their properties. This can be achieved through the formation of *in situ* generated inorganic particles to produce organic-inorganic hybrid materials.[4–10]

PI hybrid systems offer a large potential for applications in a variety of advanced technologies, either as structural materials,[6,11] including their use as matrices for high performance composites,[12,13] or as functional materials[14] such as catalyst supports[15] and microelectronics devices.[16] Among the various approaches used to produce PI hybrids, the sol-gel route provides a unique and versatile method. It can be viewed as a two step hydrolysis-condensation reaction, starting with a metal alkoxide to produce hydroxyl groups followed by the polycondensation of the hydroxyl groups and residual alkoxy groups to form a three-dimensional network.[5,17–21] Polyimide are particularly suited for this type of process because they can be obtained from polyamic acid precursors, which are soluble in hygroscopic solvents and can, therefore, tolerate the addition of water necessary to bring about the hydrolysis of the alkoxide. Moreover, the outstanding thermal stability of polyimides allows the hybrids to be post-cured at very high temperatures (300–350 °C) making it possible the development of a very dense inorganic network without inducing appreciable degradation of the organic phase.

In the present study polyimide/silica hybrid materials were prepared by the sol-gel route, and investigated with respect to their morphology, dynamic-mechanical properties, tensile and fracture behaviour.

Institute of Chemistry and Technology of Polymers (ICTP), National Research Council of Italy, Via Campi Flegrei 34, 80078 Pozzuoli (Naples), Italy
E-mail: rago@ictp.cnr.it

Different morphologies were obtained by preventing premature phase separation of the inorganic component. In particular, micron sized particulate composites were produced by using a free silica precursor (e.g., tetraethoxysilane, TEOS), while nano-structured, co-continuous morphologies were obtained by introducing a functional alkoxysilane coupling agent such as the γ-glycidyloxypropyltrimetoxysilane (GOTMS) in the precursor solution for the silica phase.

Experimental Part

The polyimide precursor used in this study was a polyamic acid, Pyre-ML RK 692 from I.S.T (Indian Orchard, MA). This has molecular weights $\overline{M}_w = 10 \cdot 10^5$, and $\overline{M}_n = 4.6 \cdot 10^4$, and is supplied as a 12 wt% solution in a mixture of N-methyl-2-pyrrolidone (NMP) and xylene (weight ratio 80/20).

The polyamic acid is obtained by condensation of pyromellitic dianhydride (PMDA) and oxydianiline (ODA). High purity grade of tetraethoxysilane (TEOS) and γ-glycidyloxypropyltrimetoxysilane, (GOTMS) were obtained from Aldrich (Milwaukee, WI). Distilled water was used to induce hydrolysis of the alkoxysilane components using a 32 wt% HCl solution as catalyst and ethanol as solvent. The alkoxysilane solutions used for the production of the polyimide/silica hybrid films were prepared from pure TEOS or TEOS/GOTMS mixtures. In a typical formulation (22.3 wt% of silica) 3.46 g of TEOS, 0.86 g of EtOH, 1.20 g of GOTMS, 0.82 g of H_2O and 1.2 g of an aqueous HCl solution (2.0 wt%) were added sequentially in a glass vial. The mixture was magnetically stirred at room temperature (RT), until a clear solution was obtained. The precursor hybrid solution was subsequently obtained by adding dropwise the hydrolysed alkoxysilane solution to the polyamic acid solution, under continuous stirring for 10 min at RT. The mixture was then used for the production of 40 μm thick films. These were prepared by spreading the solution onto a glass plate with the aid of a Gardner knife. The films were allowed to dry first for 1 h at RT and then for 1 h at 80 °C under atmospheric pressure. Finally the samples were cured stepwise at 100, 150, 200, 250 and 300 °C for 1 h at each temperature. The cured films were peeled off from the glass substrate by immersing in distilled water at 80 °C.

The morphology of the samples was examined on fractured films by scanning electron microscopy (SEM). The apparatus used was a Philips SEM mod. XL20 and the fracture surfaces were coated with a gold-palladium layer by vacuum sputtering.

Dynamic mechanical tests were carried out using a Perkin Elmer Pyris Diamond DMA apparatus. From the prepared films, rectangular samples 50 mm long, 10 mm wide and 40 μm thick were cut by a razor blade. The experiments were performed in tensile mode at frequencies of 0.1, 0.5, 1.0, 2.0, 5.0 and 10 Hz at a heating rate of 3 °C min^{-1} and a temperature range from −150 to +500 °C. The storage modulus (E′) and loss tangent (tanδ) were recorded.

For tensile measurements, dumb-bell shaped specimens with a length of 20 mm and a width of 3.5 mm were cut from the 40 μm thick films. The specimens were tested at a cross-head speed of 1 mm min^{-1} and at RT using an Instron instrument mod. 4505.

Fracture toughness measurements were performed using the Essential Work of Fracture (EWF) method. Specimens 20 mm wide, 0.04 mm thick and 100 mm long were sharply notched to produce a series of double edge-notched samples having ligament lengths, *L*, from 3 to 15 mm. The specimens were tested to complete fracture in a temperature range from ambient temperature to 250 °C, using the same equipment and cross-head speed employed for tensile tests.

Results and Discussion

Morphology

The influence of the addition of the coupling agent γ-glycidyloxypropyltrimetoxysilane,

(GOTMS) on the morphology of PI/silica hybrids has been investigated in detail. The SEM micrographs of Figure 1 for PI hybrids with 22.3 wt% of silica illustrate the compatibilization effect of GOTMS, which brings about a morphological transformation from a dispersed particle microstructure (Figure 1A), in absence of GOTMS, to a finely interconnected or co-continuous morphology (Figure 1B), with the use of GOTMS. For the compatibilized system the size of the interconnected silica domains ranges from 40 to 100 nm, while for the non compatibilized system, the average diameter of the silica particles varies from 0.8 to 1.2 μm. These morphologies are the result of a typical phase separation by spinodal decomposition[22,23] differing from each other in the extent of phase connectivity. The way through which the coupling agent induces and controls the evolution of the morphology in these hybrids was attributed to interactions, possibly by hydrogen bonding, taking place between the epoxy groups of GOTMS and the acid groups of the PI precursor.[8] These interactions delay the onset of phase separation, which results in a higher viscosity of the solution and in a reduction of the rate of particle growth.[5,8] It has been found that a threshold value of the GOTMS/TEOS molar ratio exists for the formation of co-continuous morphologies.[24]

This threshold value was found to change with the total silica content in the hybrid. For a silica concentration of 22.3 wt%, calculated theoretically assuming

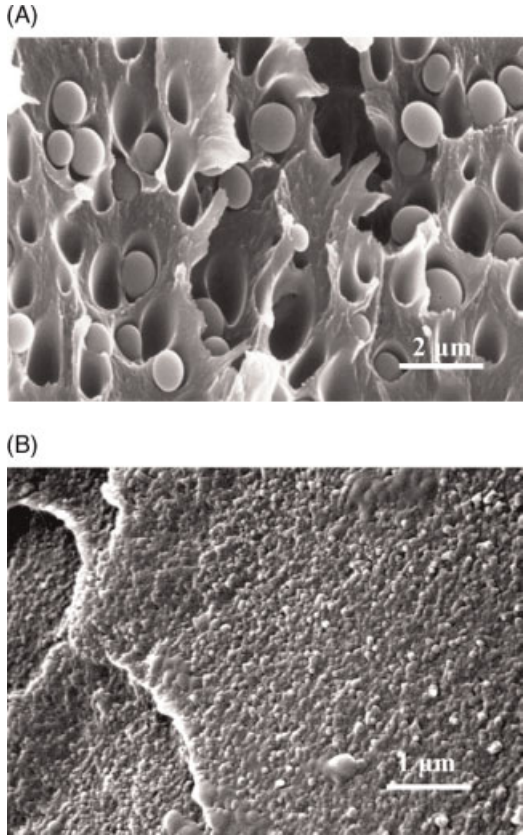

Figure 1.
SEM micrographs of polyimide/silica hybrids with 22.3 wt% of silica: A) hybrid without the GOTMS coupling agent; B) hybrid with the GOTMS coupling agent.

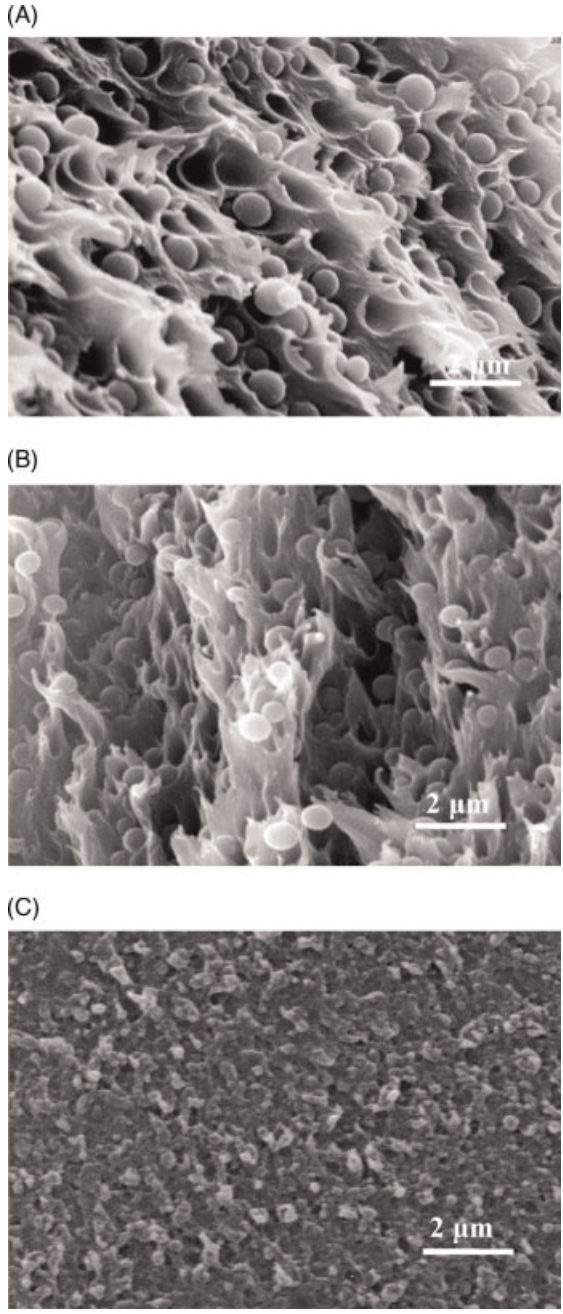

Figure 2.
SEM micrographs of PI/silica hybrids with different GOTMS/TEOS molar rations: A) GOTMS/TEOS 0.02; B) GOTMS/TEOS 0.03; C) GOTMS/TEOS 0.1.

complete conversion of TEOS and GOTMS to silica, the threshold GOTM/TEOS molar ratio is located between 0.06 and 0.08.

In Fig. 2 are shown the SEM micrographs of hybrids having 22.3wt% of silica and different GOTMS/TEOS values. For molar rations lower than the limiting value,

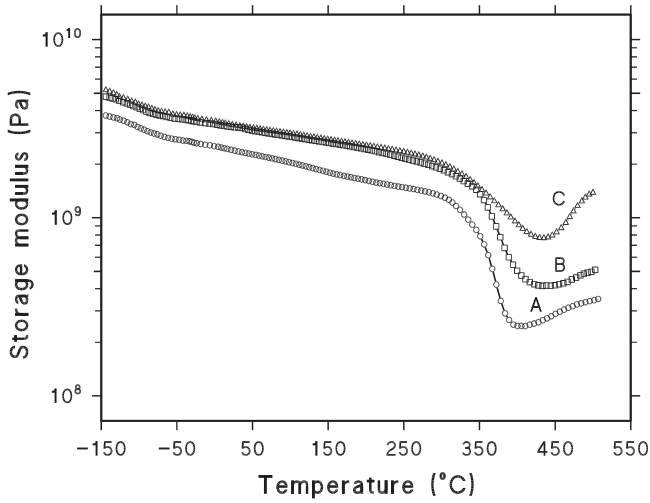

Figure 3.
Storage modulus as a function of temperature: A) pure polyimide; B) microcomposite with 22.3 wt% of silica; C) nanocomposite with 22.3 wt% of silica.

the hybrids display (Figures 2A and 2B) a particulate morphology like that of Figure 1A, but with smaller particles sizes. The dimensions of the silica particles decrease from about 0.61 μm to 0.32 μm with increasing the amount of GOTMS. The micrograph of Figure 2C, on the other hand, illustrates the morphology obtained with a GOTMS/TEOS molar ration slightly above the threshold value. This morphology is close to that of Figure 1B for which a higher GOTMS concentration was used. TEM examinations for the co-continuous structures revealed additional morphological features.[24] In particular, it was found that increasing the GOTMS/TEOS molar ration above the threshold value had the effect of reducing the size of the silica domains. Thus the GOTMS/TEOS molar ratio represents a parameter which allows us to finely tune the size of the silica particle in the system. This flexibility in the management of the final morphology permits to realize PI/silica hybrids tailored to specific requirements.

Dynamic Mechanical Properties

The storage modulus (E′) and the loss factor tan δ for the pure PI, and for two hybrids, one with a particulate micron sized structure (microcomposite) and the other with a nano-structured, co-continuous morphology (nanocomposite), are shown, respectively, in Figures 3 and 4.

The presence of silica increases the elastic modulus both in the glassy region and at temperature above the glass transition. The upturn in the storage modulus curves above the glass transition is likely to result from intermolecular crosslinking reactions. The tan δ plots (Figure 4) reveal the occurrence of three relaxation processes: the low and the medium temperature relaxations are defined, respectively, as the γ and β transition (Figure 4a). The high temperature peak is a α-relaxation process and corresponds to the glass transition temperature (Figure 4b). The β transition displays an asymmetrical shape and occurs over a very wide temperature range. It has been generally associated with local bond rotations along the polyimide backbone, although its exact description is still uncertain.[25–28] The lowest-temperature γ transition has been observed previously in a limited number of studies and only in the presence of absorbed moisture.

From the data of Figure 4, two observations can be made with respect to the incorporation of the silica phase within the polyimide matrix. The first is that the γ, β and α peaks are displaced toward higher

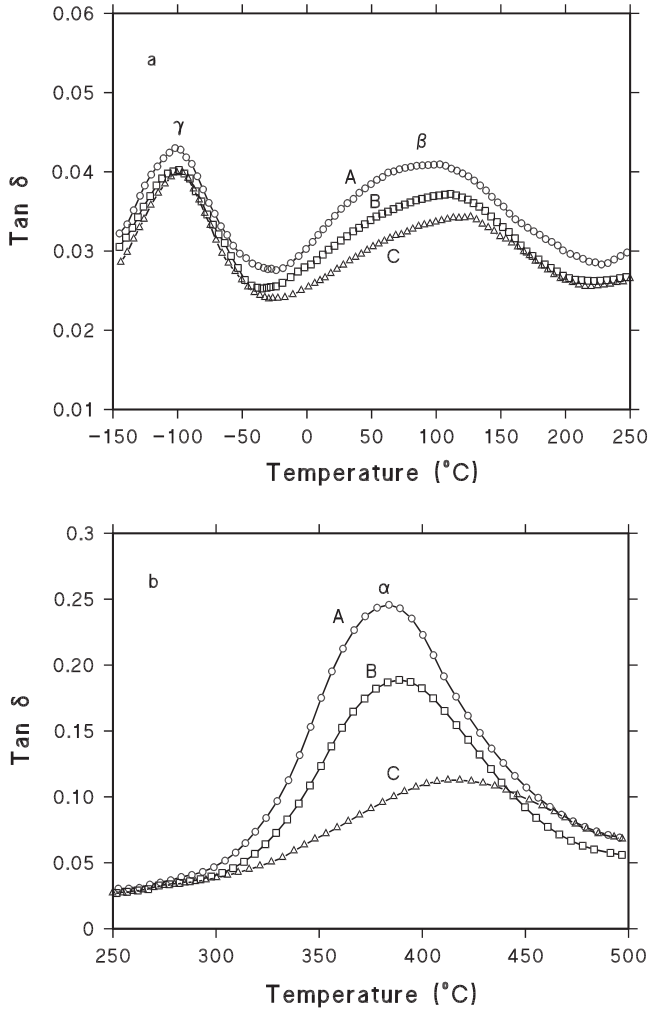

Figure 4.
Tan δ spectra as a function of temperature: A) pure polyimide; B) microcomposite with 22.3 wt% of silica; C) nanocomposite with 22.3 wt% of silica. 4a: temperature range −150–250 °C; 4b: temperature ranges 250–500 °C.

temperatures. The increase in T_β and T_α is about 10 °C for the microcomposite and, respectively, of 24 °C and 34 °C for the nanocomposite. The T_γ increase is considerably lower. The second observation is that the height of these transitions decreases. The effect is larger for the β and α processes and is much more pronounced for the nanocomposite sample.

Further details on the effect of the silica phase on the γ, β and α transitions were gathered by a multi-frequency analysis. It was found that, by increasing the frequency, the peak maxima of these relaxation processes shifted at higher temperature, while the intensities decreased. This frequency dependence was examined using the Arrhenius equation:

$$f = A \cdot e^{\frac{-Ea}{RT}}$$

where f is the frequency, A is the pre-exponential factor, R is the gas constant, T is the absolute peak temperature and E_a is the activation energy.

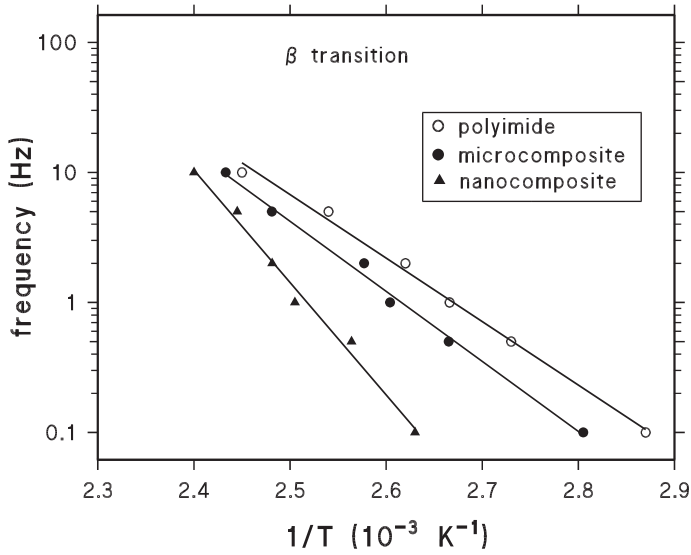

Figure 5.
Arrhenius plot relative to the β transition for the PI, the microcomposite and the nanocomposite.

The above equation has been employed to evaluate the activation energies of the γ, β and α transitions of the PI/silica hybrids and the parent PI. In Figure 5 is reported the logarithm of frequency as a function of 1/T for the β relaxation process. Analogous diagrams were obtained for the γ and α transitions.

The activation energies, determined from the slope of Arrhenius plots, are summarized in Table 1. For the microcomposite the values differ slightly from those of the pure PI, while a significant enhancement is found for the nanocomposite, especially for the activation energies related to the β and α transitions.

These results point to an increased constrain on the mobility of chain segments due to the occurrence of interactions between the silica phase and the polyimide matrix. Such interactions are stronger for the nanocomposite owing to the action of GOTMS coupling agent. Thus a co-continuous morphology is much more effective in depressing the molecular motions of the polyimide chains with respect to a micron sized, particulate structure. In accordance with the dynamic-mechanical results, larger reductions in the coefficient of thermal expansion were found when the morphology changed from particulate to co-continuous.[11]

Tensile and Fracture Properties

Typical tensile stress-strain curves for PI/silica hybrids with a silica content of 15.0 wt% and for the parent polyimide are shown in Figure 6. The neat PI (curve A) exhibits an extensive yielding and strain hardening before fracture. A similar behaviour is observed for the microcomposite sample (curve B), while the nanocomposite

Table 1.
γ, β and α activation energies for PI and PI/silica hybrids.

Sample	γ E_a (kcal/mol)	β E_a (kcal/mol)	α E_a (kcal/mol)
Polyimide	10.3	22.7	240.1
Microcomposite	10.0	24.9	252.0
Nanocomposite	11.7	36.9	284.3

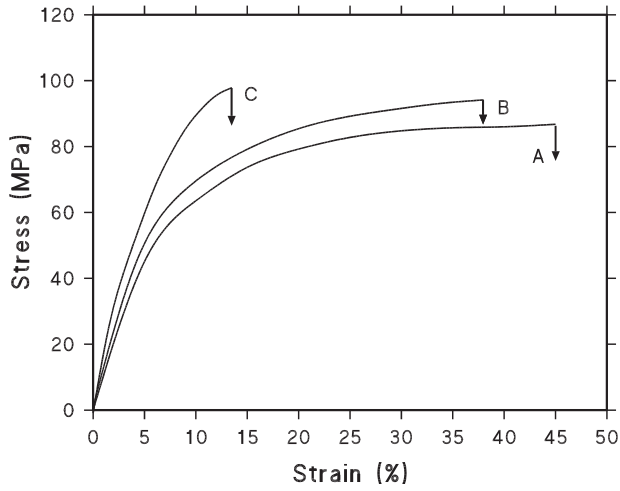

Figure 6.
Typical stress-strain curves of PI/silica hybrids. Curve A: plain PI; Curve B: microcomposite with 15.0 wt% of silica; Curve C: nanocomposite with 15.0 wt% of silica.

(curve C) shows a fracture that takes place prior to yielding.

The properties derived from the stress-strain diagrams of Figure 6 are reported in Table 2. The PI/silica hybrids show a higher modulus and strength with respect to the pure polyimide, reflecting the reinforcing effect of the inorganic phase. However, this enhancement is larger for the nanocomposite as the result of both a better interfacial adhesion and the formation of a co-continuous morphology. In spite of the enhanced adhesion the nanocomposite exhibits a strong reduction in the elongation at break if compared to both the microcomposite and the plain polyimide. This brittle behaviour has been attributed to the interconnected silica phase that hinder the plastic flow of the polyimide matrix, preventing large deformations to take place before fracture.

The ductile fracture mode exhibited by the pure polyimide and the hybrids with a micron sized particulate morphology was investigated by means of the Essential Work of Fracture (EWF) method. Recent studies[29–31] have shown that this approach represents an useful tool for determining the toughness of ductile polymers in the form of very thin films. This method was found unsuitable for nanosized hybrids owing to their fragile behaviour.

Figure 7 shows the fracture toughness, expressed in term of the essential work of fracture parameter, w_e, versus temperature for a series of particulate PI/silica hybrids and for the pure polyimide. The parameter, w_e, is found to increase linearly with increasing temperature and, at any given temperature, the enhancement of fracture toughness is related to the silica content. It is also found (see Table 3) that, for a given silica content, the fracture toughness increases further when the GOTMS coupling agent is added to the silica precursor.

Table 2.
Tensile mechanical parameters for PI/silica hybrids with 15.0 wt% of silica.

Sample	Modulus (GPa)	Tensile strength (MPa)	Elongation at break (%)
Polyimide	1.9	86.3	44.6
Microcomposite	2.5	92.2	38.3
Nanocomposite	2.9	98.4	13.4

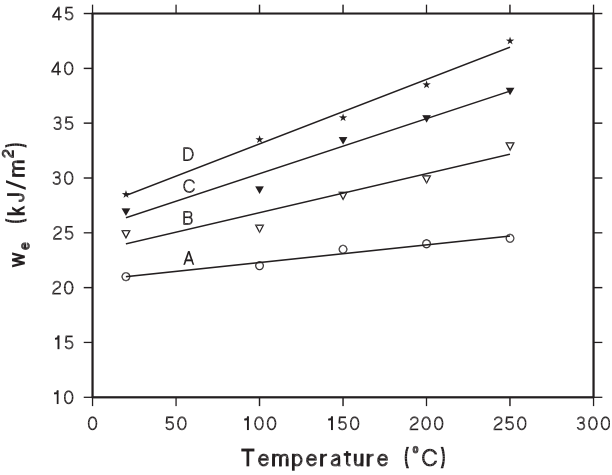

Figure 7.
Essential work of fracture, w_e, as a function of temperature: A) polyimide; B) microcomposite with 10 wt% of silica; C) microcomposite with 15 wt% of silica; D) microcomposite with 20 wt% of silica.

The fractographic analysis (Figure 8) shows that the fracture process of these hybrids is dominated by interface-initiated cavitations. This mechanism is known to occur in particulate composites with spherical particles when the matrix modulus is lower than that of the particles.[31] In particular, due to the poor adhesion between particles and matrix, a debonding process takes place at both equator and pole regions of the particles. The debonding of the matrix from the particles relaxes the local interfacial stresses promoting shear yielding mechanisms. Thus cavitations and matrix yielding are the deformation mechanisms responsible for the enhancement in the fracture toughness observed for micron sized, particulate PI/ silica hybrids. The addition of GOTMS (compare Figure 8A with Figures 8B and 8C) reduces the particles diameter and improves the interfacial strength, thus favouring the conditions for promoting shear yielding processes in the PI matrix. Accordingly, higher values of w_e are found with respect to that in absence of GOTMS.

Conclusions

Several polyimide/silica hybrids have been prepared and characterized with respect to their morphology, relaxation processes and tensile and fracture properties. A sol-gel type process has been employed to produce co-continuous nanocomposite structures or more conventional, two-phase micron sized composites. It has been shown that the sol-gel process was a versatile tool for the production of such hybrids since it allows a considerable control on the final morphology. In particular, the GOTMS/TEOS molar ratio was found to be the key factor in determining the size of the silica particles

Table 3.
The essential work of fracture, w_e, for microcomposites with 15.0 wt% of silica containing different GOTMS/TEOS molar rations.

Silica content (wt%)	GOTMS/TEOS (molar ratio)	w_e (kJ/m^2)	Temperature (°C)
15.0	0.0	26.5	20
15.0	0.03	28.2	20
15.0	0.04	30.4	20

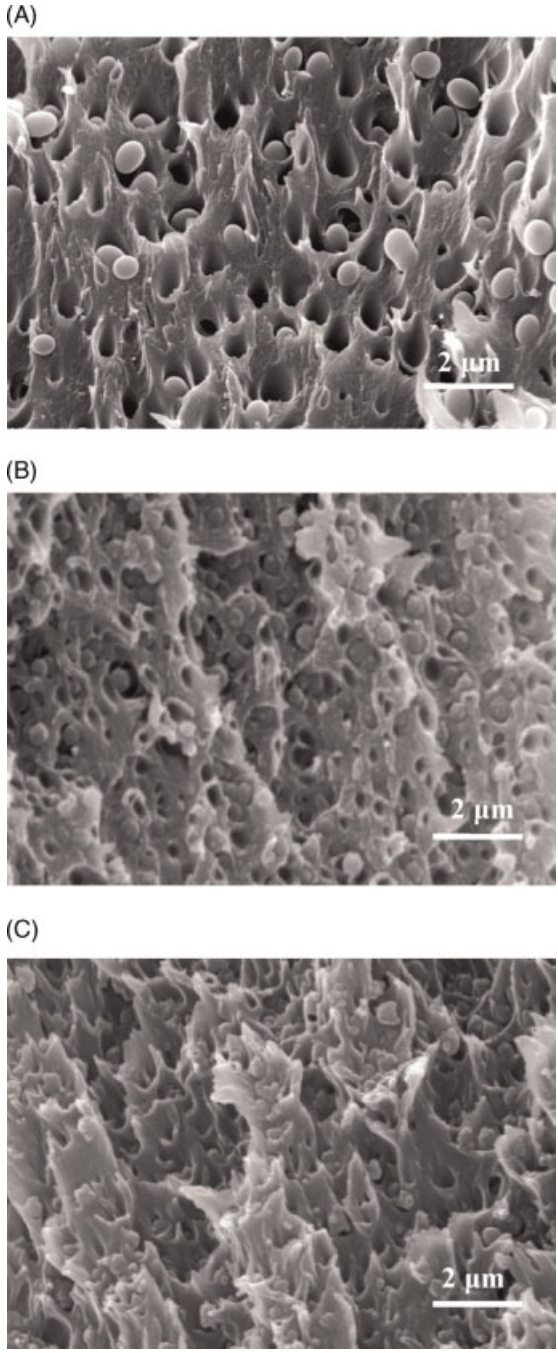

Figure 8.
SEM micrographs of fractured surfaces at ambient temperature of PI/silica hybrids with 15.0 wt% of silica containing different GOTMS/TEOS molar rations: A) GOTMS/TEOS 0.0; B) GOTMS/TEOS 0.03; C) GOTMS/TEOS 0.04.

in the system. The relaxation processes of the polyimide have been found to be strongly influenced by the presence of the inorganic phase when an interconnected co-continuous system is realized. Much lower effects were observed in the case of conventional two-phase systems. The lowering of the transition peaks and the increase of the activation energies found for nanocomposite samples were attributed to interactions between the two phases due to the action of the GOTMS coupling agent. Also the mechanical properties were strongly dependent on the system morphology. The co-continuous structure showed an increased modulus and strength, but a lower elongation at break with respect to both the plain polyimide and the micron sized hybrids. However, the latter systems showed enhanced ductility and fracture toughness since the dispersed silica particles induced interfacial cavitations and shear yielding of the polyimide matrix. The extent of these deformation mechanisms was found dependent on the silica content, interfacial strength and temperature.

[1] C. M. K. Gosh, K. L. Mittal, *Polyimides: Fundamentals and Applications*, Marcel Dekker, New York **1996.**
[2] M. I. Bessonov, V. A. Zubkov, *Polyiamic Acids and Polyimides: Synthesis, Trasformation and Structure*, CRC Press, Boca Raton **1993**.
[3] L. F. Thompson, C. G. Willson, S. Tagawa, *Polymers for microelectronics: Resists and Dielectrics*, ACS Symposium Series 537, Washington, DC **1994**.
[4] J. E. Mark, C. Y. C. Lee, P. A. Bianconi, *Hybrids Organic-Inorganic Composites*, ACS Symposium Series 585, Washington, DC **1995**.
[5] A. Kiul, L. Mascia, *J. Non-Cryst. Solid* **1994,** *175*, **169.**
[6] L. Mascia, *Trends Polym. Sci.* **1995**, *3*, 61.
[7] A. Marikawa, Y. Iyoku, M. Kakimoto, Y. Imal, *Polym. J.* **1992**, *24*, 107.
[8] P. Musto, G. Ragosta, G. Scarinzi, L. Mascia, *Polymer* **2004**, *45*, 4265.
[9] G. Ragosta, P. Musto, M. Abbate, P. Russo, G. Scarinzi, *Macromol. Symp.* **2005**, *228*, 287.
[10] P. Musto, G. Ragosta, G. Scarinzi, L. Mascia, *Polymer* **2004**, *45*, 1697.
[11] L. Mascia, A. Kiul, *Polymer* **1995**, *36*, 3649.
[12] J. E. Mark, *Polym. Eng. Sci.* **1996**, *36*, 2905.
[13] L. Mascia, Z. Zhang, S. J. Shaw, *Composites* **1996**, *27A*, 1211.
[14] Y. Wei, J. M. Yeh, D. Jin, X. Jia, J. Wang, G. W. Jang, *Chem. Mater.* **1995**, *7*, 979.
[15] C. G. Guizard, A. C. Julbe, A. J. Ayral, *Mat. Chem.* **1999**, *9*, 55.
[16] J. Kang, D. J. Lee, S. K. Choi, H. K. Kim, *Mol. Cryst. Sci. Technol. Sect.* **1996**, *280*, 277.
[17] M. Nadi, J. A. Conklin, L. SalvatiJr., A. Sen, *Chem. Mat.* **1991**, *3*, 201.
[18] G. L. Wilkes, B. Order, H. H. Huang, *Polym. Bull.* **1985**, *14*, 557.
[19] C. J. Wung, Y. Pang, P. N. Prasad, F. E. Karaz, *Polymer* **1991**, *32*, 65.
[20] C. J. T. Landry, B. K. Coltrain, B. K. Brady, *Polymer* **1991**, *32*, 65.
[21] L. Mascia, A. Kiul, *J. Mat. Sci.* **1994**, *13*, 641.
[22] T. Inoue, *Prog. Polym. Sci.* **1995**, *20*, 119.
[23] K. Yamanaka, Y. Takagi, T. Inoue, *Polymer* **1989**, *30*, 1839.
[24] J. D. C. Menomo, L. Mascia, S. J. Shaw, *Mat. Res. Soc. Symp. Proc.* **1996**, *435*, 199.
[25] R. M. Ikeda, *J. Polym. Sci. Polym. Lett. Ed.* **1996**, *4*, 353.
[26] Y. H. Kim, B. S. Moon, F. W. Harris, S. Z. D. Cheng, *J. Therm. Anal.* **1996**, *46*, 921.
[27] F. M. Li, S. Fang, J. J. Ge, P. S. Chen, F. W. Harris, S. Z. D. Cheng, *Polymer* **1996**, *40*, 4987.
[28] W. Qu, T. M. Kao, R. H. Vora, T. S. Chung, *Polymer* **2001**, *42*, 6393.
[29] S. Hashemi, *J. Mat. Sci.* **1997**, *32*, 1563.
[30] J. Karger-Kocsis, T. Czigany, J. Moskala, *Polymer* **1997**, *38*, 4587.
[31] B. Cotterell, J. K. Reddel, *Int. J. Fract.* **1997**, *13*, 267.

